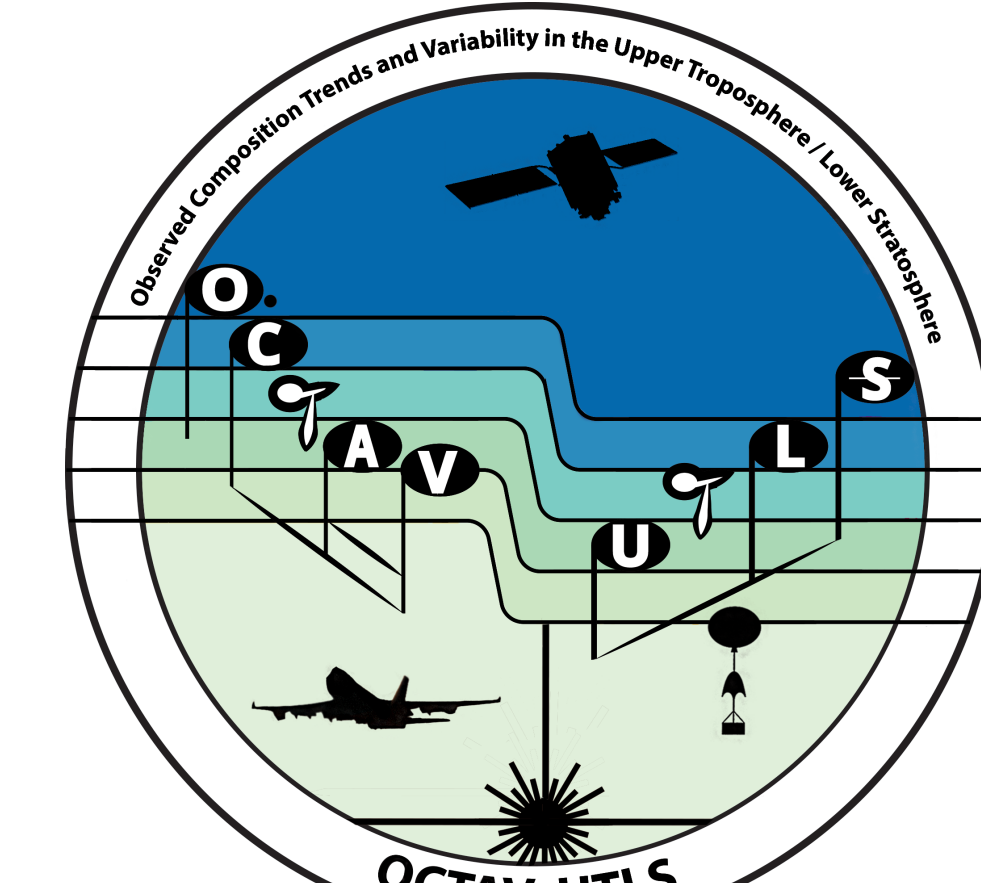


How do UTLS jet and tropopause dynamics influence ozone variability? Investigations supporting the SPARC OCTAV-UTLS Activity

Gloria L Manney, Luis F Millán Valle, Harald Boenisch, Adam Bourassa, Michaela I Hegglin, Peter Hoor, Paul S Jeffery, Daniel Kunkel, Zachary D Lawrence, Nathaniel J Livesey, Mark A Olsen, Irina Petropavlovskikh, Kaley Walker, Krzysztof Wargan



Motivation: UTLS Ozone Evolution, OCTAV-UTLS, and JETPAC

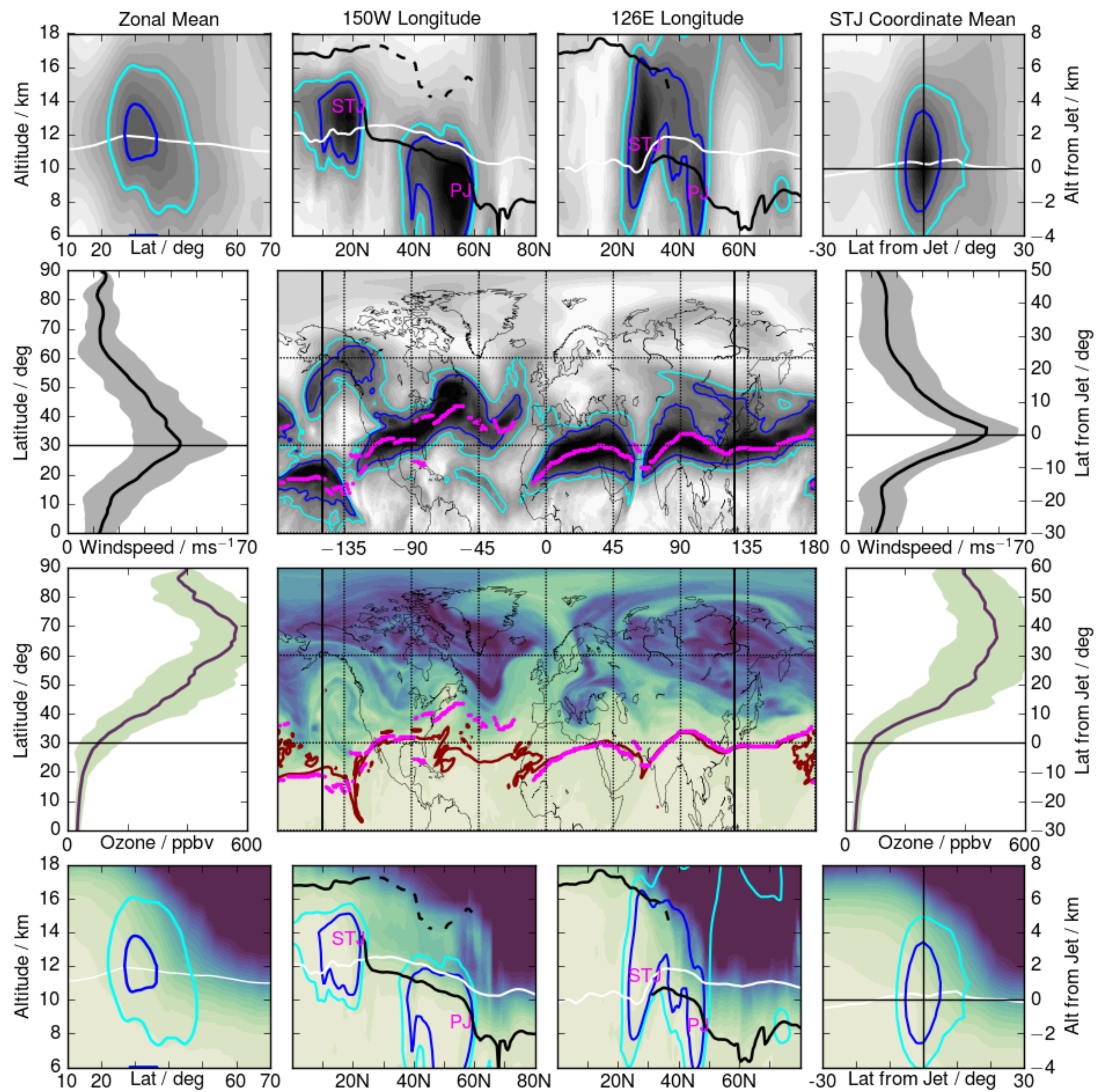


Figure 1: Example (central maps) 345 K windspeed and ozone fields from MERRA-2 on 29 January 2009, with vertical cross-sections shown above and below. Plots to the left show zonal means of these fields, and those to the right show the fields mapped in subtropical jet (STJ) relative coordinates using JETPAC (Jet and Tropopause Product for Analysis and Characterization, Manney et al., 2011, 2014, 2017; Manney and Hegglin, 2018).

Observed Composition Trends And Variability in the UTLS (OCTAV-UTLS) SPARC Activity goals include:

- Utilize multi-platform composition measurements
- Use Geophysically-based coordinate systems
- Provide guidance on measurement usage and needs for UTLS trend studies

First stages of OCTAV-UTLS include exploring different coordinate systems using JETPAC (Figure 2)...

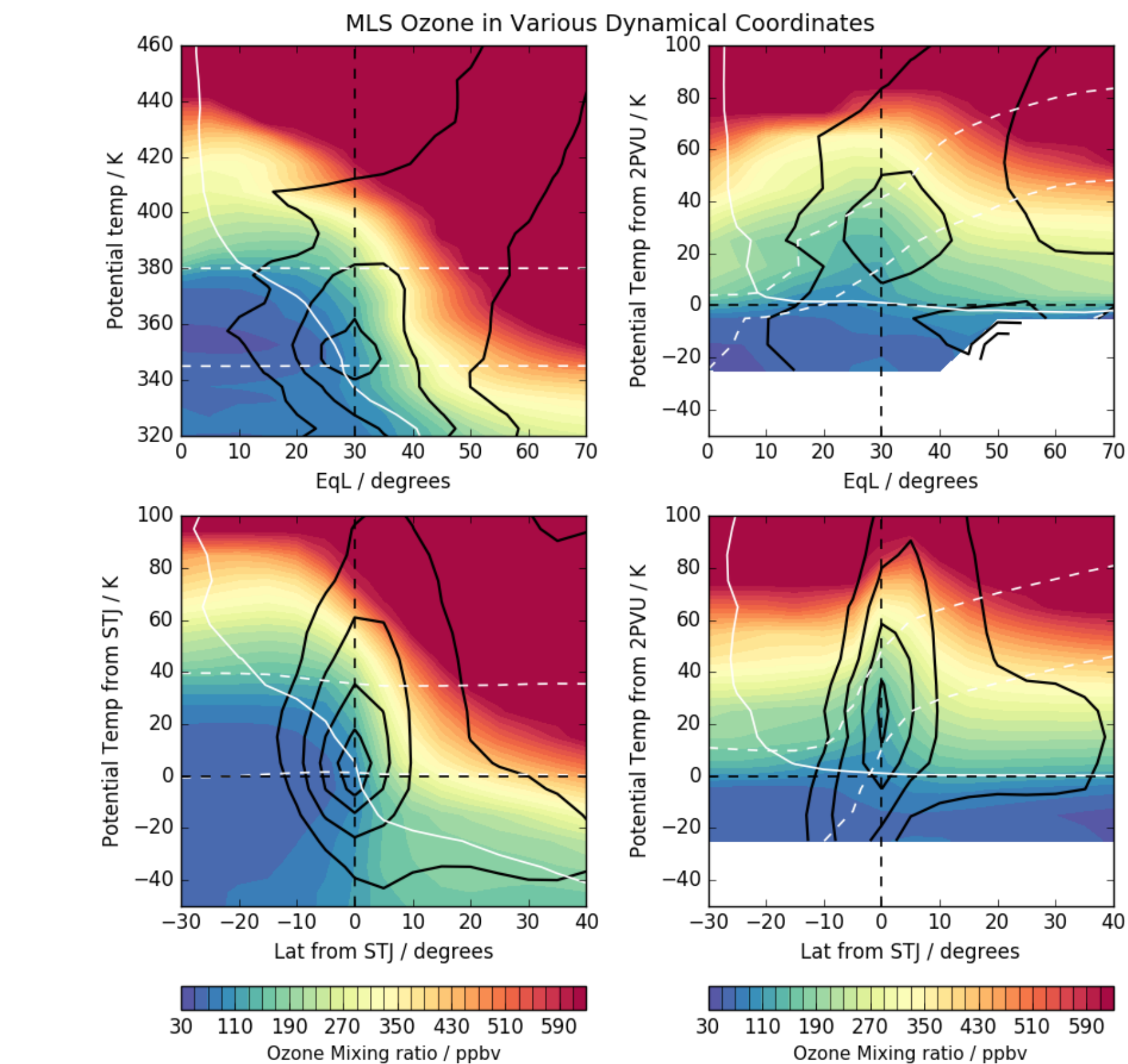


Figure 2: MLS data for DJF 2005–2016 in geophysical coordinates, with overlaid windspeeds from MERRA-2 interpolated to the MLS measurement locations (black), 2PVU PV contour (white), and 345 K and 380 K potential temperature contours (dashed white).

...and assessing mapping of multi-platform data into geophysical coordinates (Figure 3).

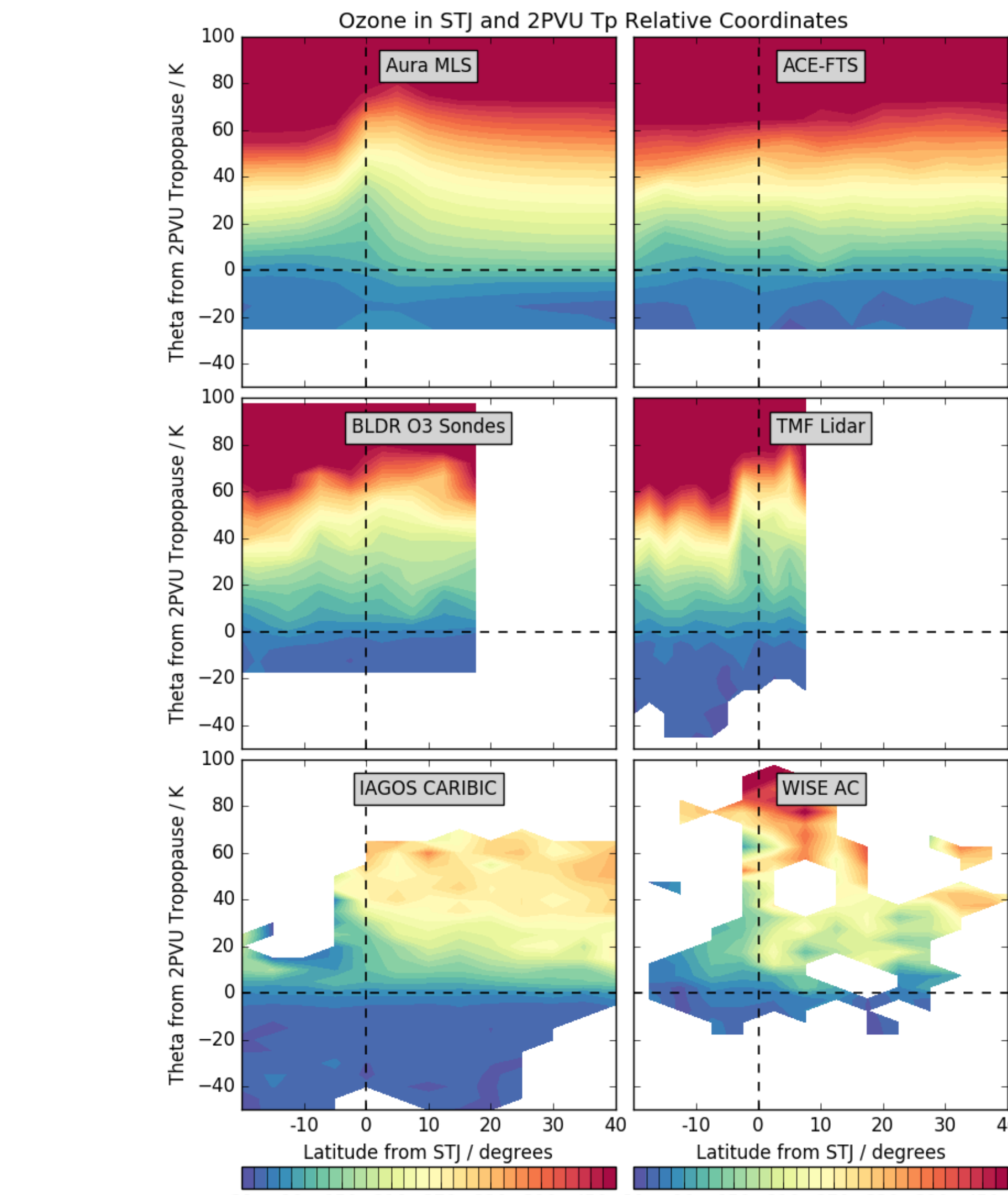


Figure 3: Multiplatform UTLS ozone mapped with respect to the distance from the STJ and distance from the 2PVU dynamical tropopause. For SON 2005–2016, except for WISE campaign, which took place in Sep–Oct 2017.

Foundations for OCTAV-UTLS include understanding mechanisms controlling the relationships of ozone to dynamical coordinate variables (in other words, effects of circulation and transport on ozone), including:

- Transport barriers and STE
- Mixing processes
- Relationships of ozone to natural modes of variability

The following panels show examples from studies planned and in progress, focusing on exploring foundations for the OCTAV-UTLS work.

S-RIP analyses: MLS and Reanalysis UTLS ozone variability

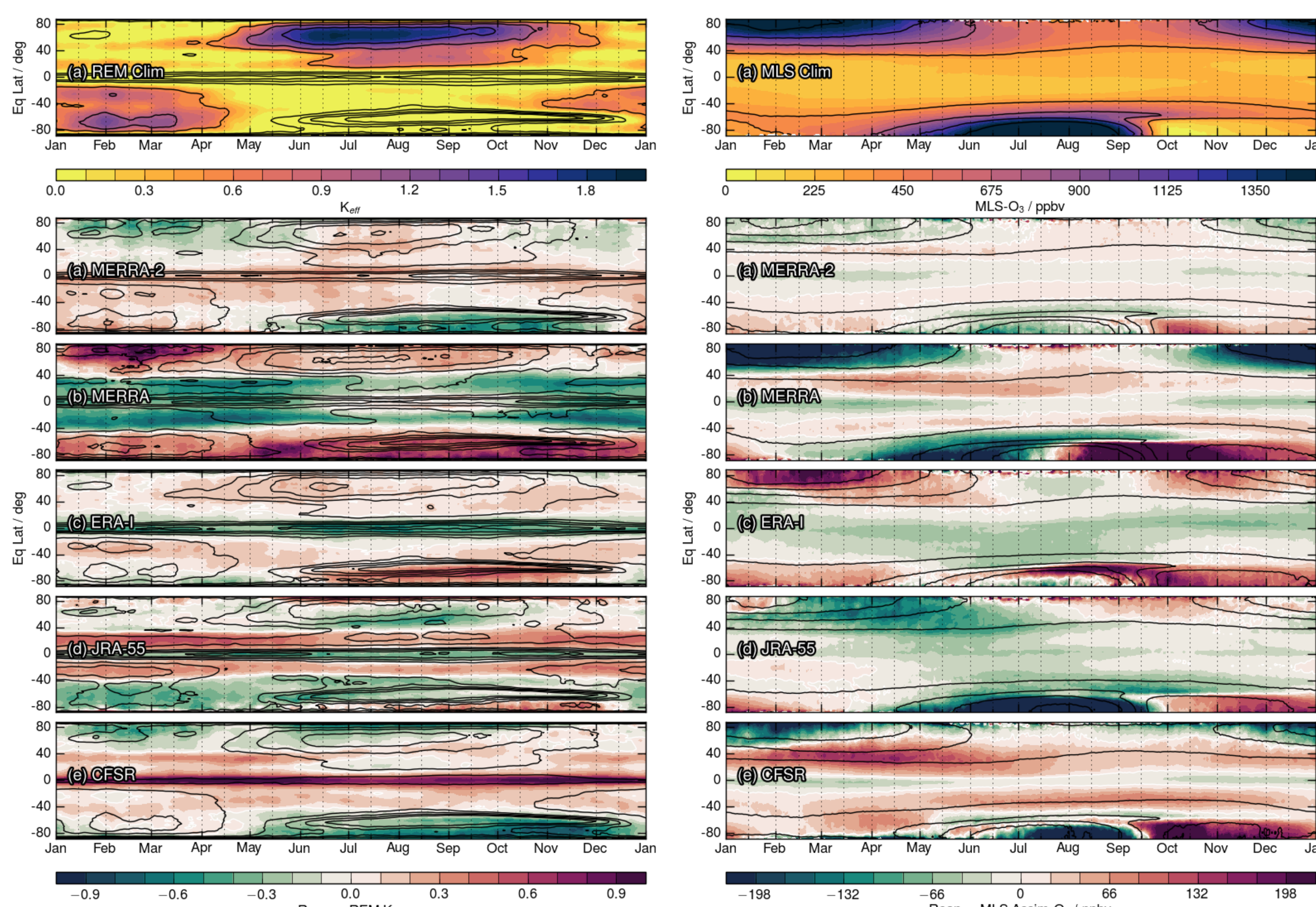


Figure 4: Comparison of climatological (1979–2015) (left) effective diffusivity (a mixing diagnostic) from five reanalyses and (right) MLS and reanalysis ozone in EqL coordinates. (From S-RIP Chapter 7 final draft, Co-leads Manney and Homeyer.)

Many SPARC-Reanalysis Intercomparison Project (S-RIP) Studies are relevant to OCTAV-UTLS, including:

- Chapter 4 Overview of Ozone and water Vapour: See Davis et al. (2017)
- Chapter 7 Extratropical UTLS: Comparisons of assimilated and MLS ozone in EqL (Figure 4) and jet-based coordinate systems (Figure 5); comparisons of reanalysis UTLS jets and tropopauses (e.g., Manney et al., 2017; Xian and Homeyer, 2019)
- Chapter 8 Tropical Tropopause Layer: Asian Summer Monsoon (e.g., Manney et al., 2019b, in preparation), STJ trends (e.g., Manney and Hegglin, 2018) and tropical width, and tropical tropopause comparisons

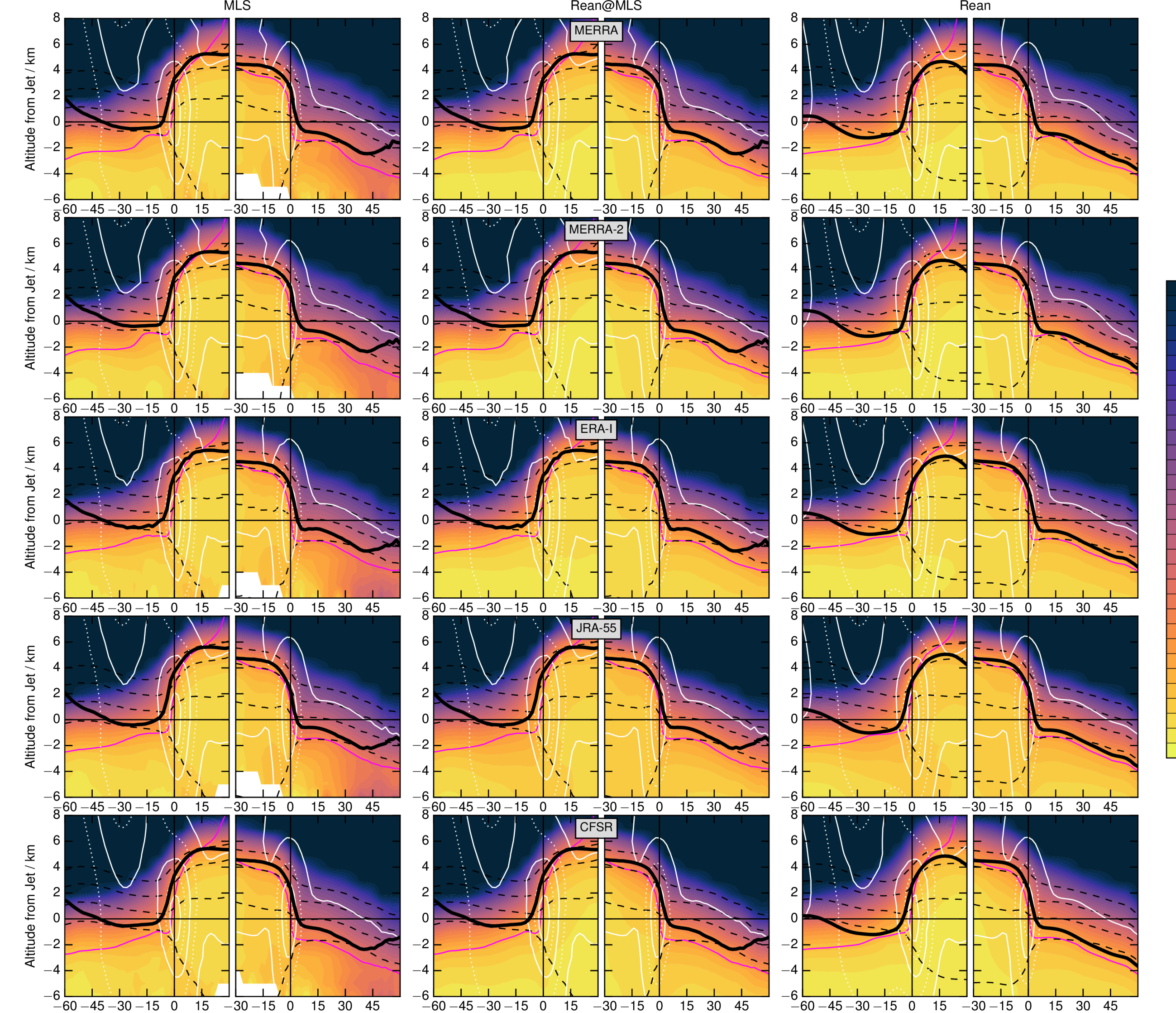


Figure 5: MLS and reanalysis ozone in coordinates relative to the STJ. Left panels show MLS ozone mapped in jet coordinates using each of the reanalyses, center panels show reanalysis ozone mapped into jet coordinates after being interpolated to MLS measurement locations, and right panels show reanalysis ozone mapped directly from their native grids. (From S-RIP Chapter 7 final draft, Co-leads Manney and Homeyer.)

RWB, Mixing, and Transport Barriers

Numerous dynamical and mixing processes related to UT jet and tropopause variations drive UTLS ozone changes.

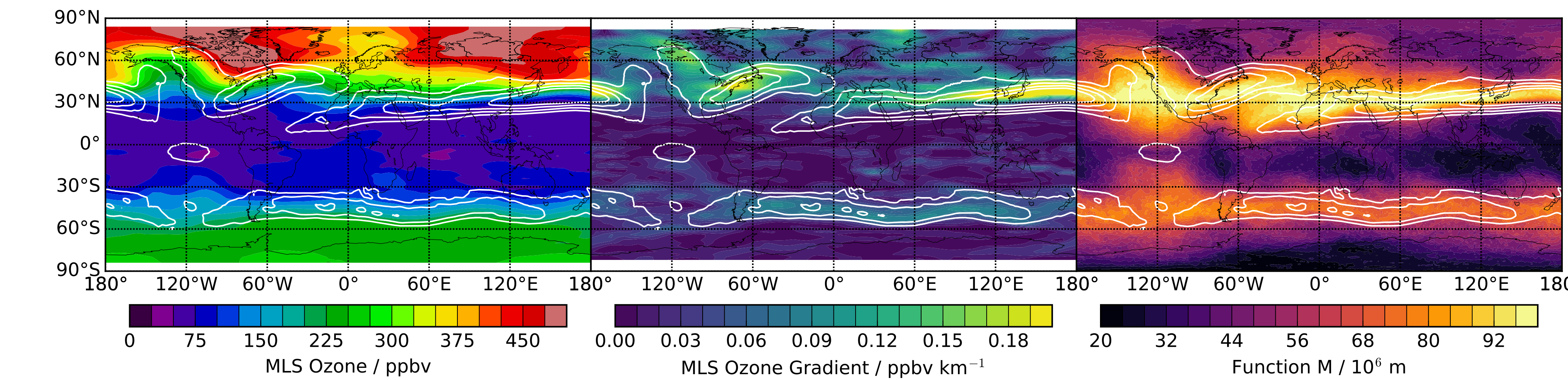


Figure 6: MLS ozone, ozone gradients, and a Lagrangian mixing diagnostic (the “Function M”) on the 345 K isentropic surface for January 2014. Black overlays are windspeeds.

These include:

- Effective diffusivity (e.g., Figure 4) and longitudinally-resolved mixing diagnostics (Figure 6 shows an example of “the Function-M” in relation to MLS ozone and ozone gradients)
- Rossby wave breaking (Figure 7)
- UT jet variability, multiple WMO gradient tropopauses (e.g., relationships with composition described in Schwartz et al., 2015), stratospheric subvortex and UT jet relationships, & multiple dynamical tropopauses (i.e., tropopause folds) (Figure 8)

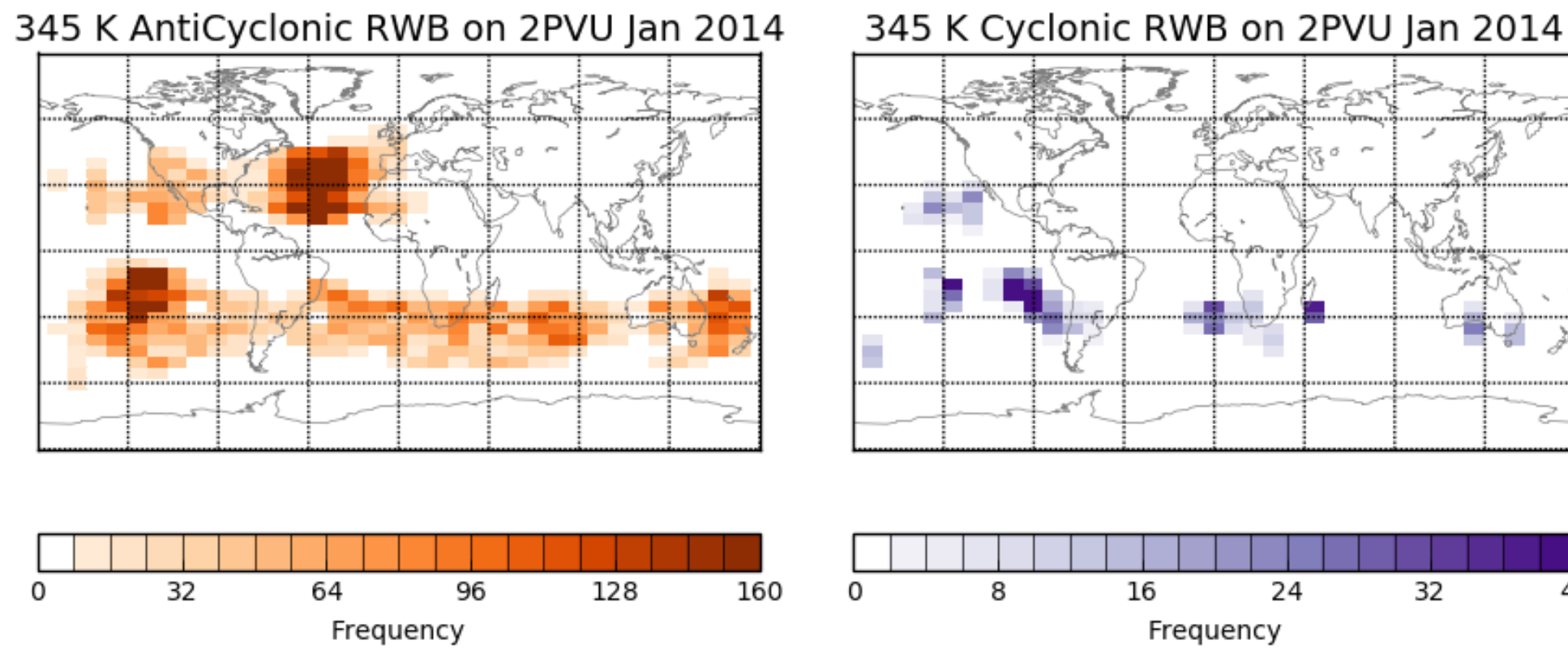


Figure 7: January 2014 anticyclonic and cyclonic Rossby wave breaking frequencies at 345 K on 2PVU contour.

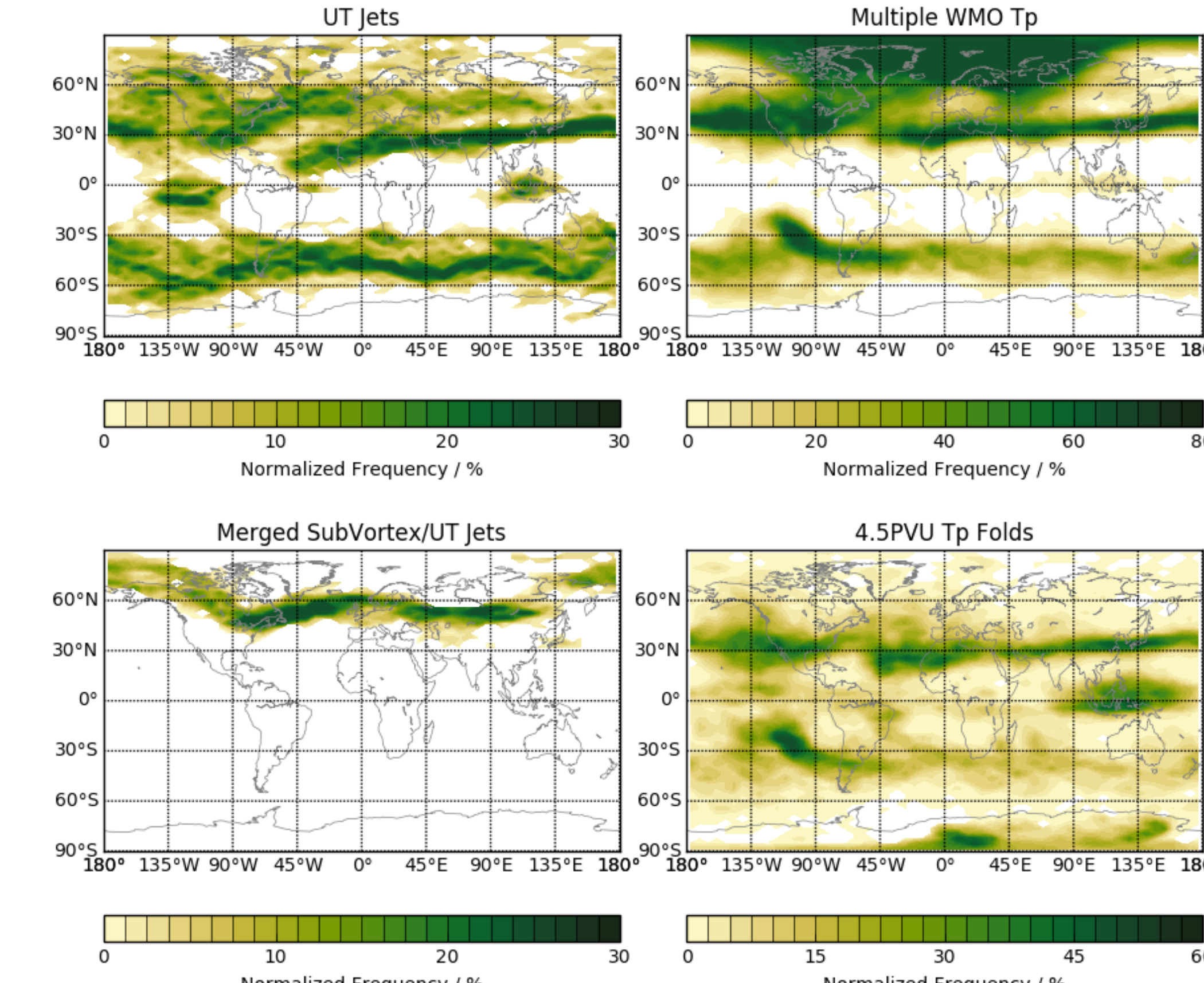


Figure 8: Example UTLS jet and multiple tropopause diagnostics for January 2014: UT jet frequencies, multiple WMO tropopauses, merged subvortex & UT jet frequencies, and folding of 4.5PVU dynamical tropopause.

Other Ongoing & Future Work

Continuing and planned studies will address in more detail:

- Relationships of ozone evolution to dynamical processes in the UTLS
- How these relationships affect the interpretation of ozone variability in dynamical coordinates (e.g., Figure 13)
- How these mechanisms are reflected in measurements with different sampling, resolution, and uncertainties

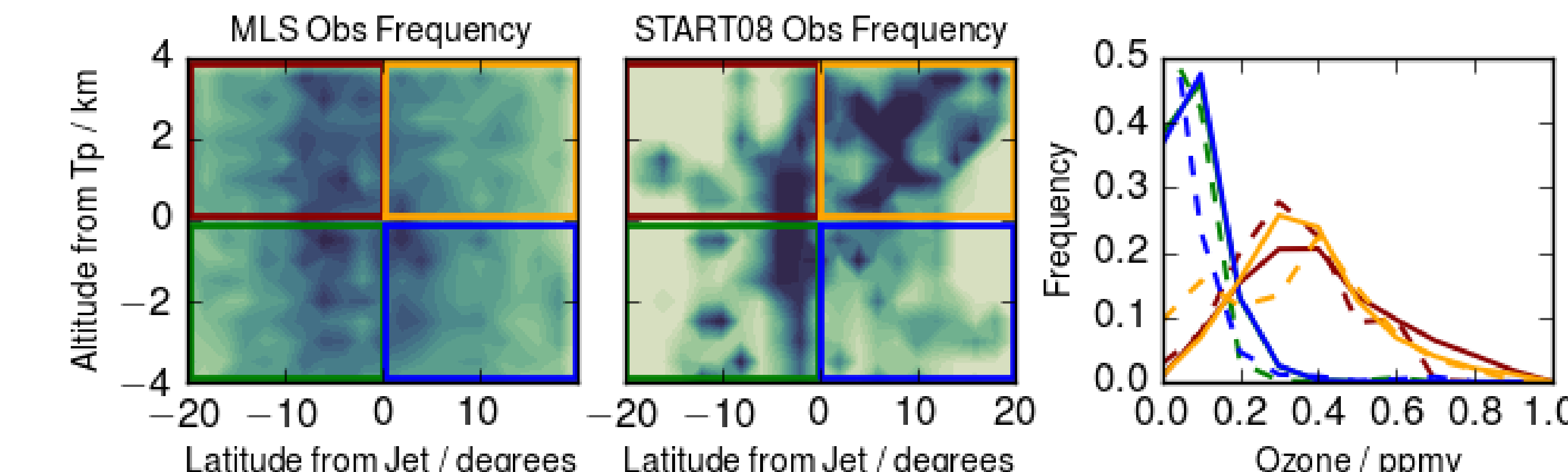


Figure 13: Comparison of MLS and START08 ozone in broad regions equatorward and poleward of the subtropical jet and above and below the tropopause.

Other ozone datasets that we are analyzing include Aura HIRDLS, SAGE II and SAGE III/ISS, Odin OSIRIS (e.g., Figure 14), and the START08 aircraft campaign (e.g., Figure 13). The techniques used for these analyses will also be applied to climate and transport models (e.g., Figure 14) to help elucidate mechanisms.

Multiyear (2010–2012) Zonal Mean O₃

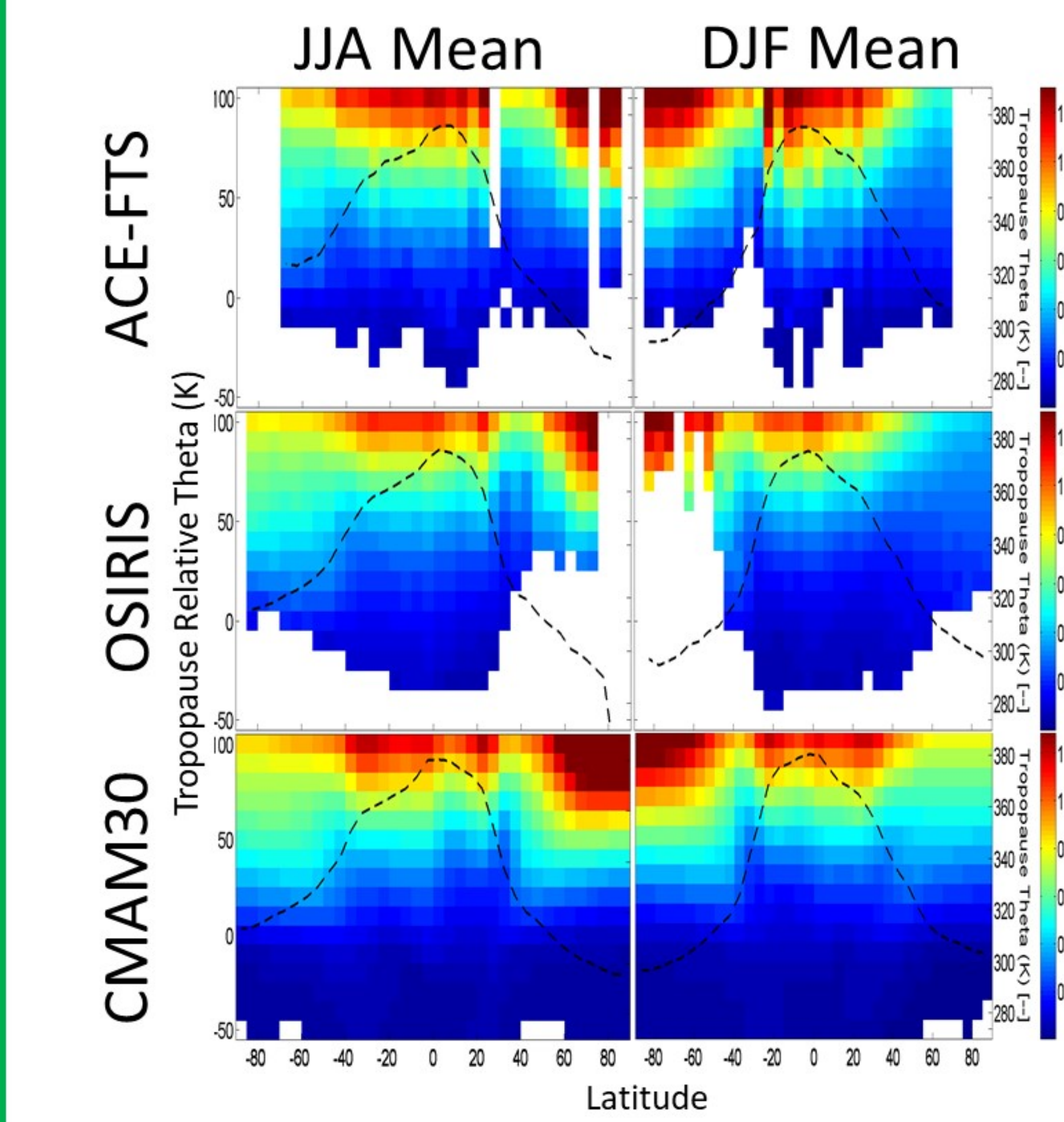


Figure 14: JJA and DJF seasonal and zonal mean ozone in coordinates relative to the 2PVU tropopause, from ACEFTS, OSIRIS, and the CMAM30 specified-dynamics simulation. Dashed black line shows the potential temperature of the 2PVU tropopause.

Relationships of Jets and Ozone to Natural Variability

Manney and Hegglin (2018) showed robust tropical widening and narrowing (measured by STJ latitude changes) in limited regions and seasons (e.g., Figure 9).

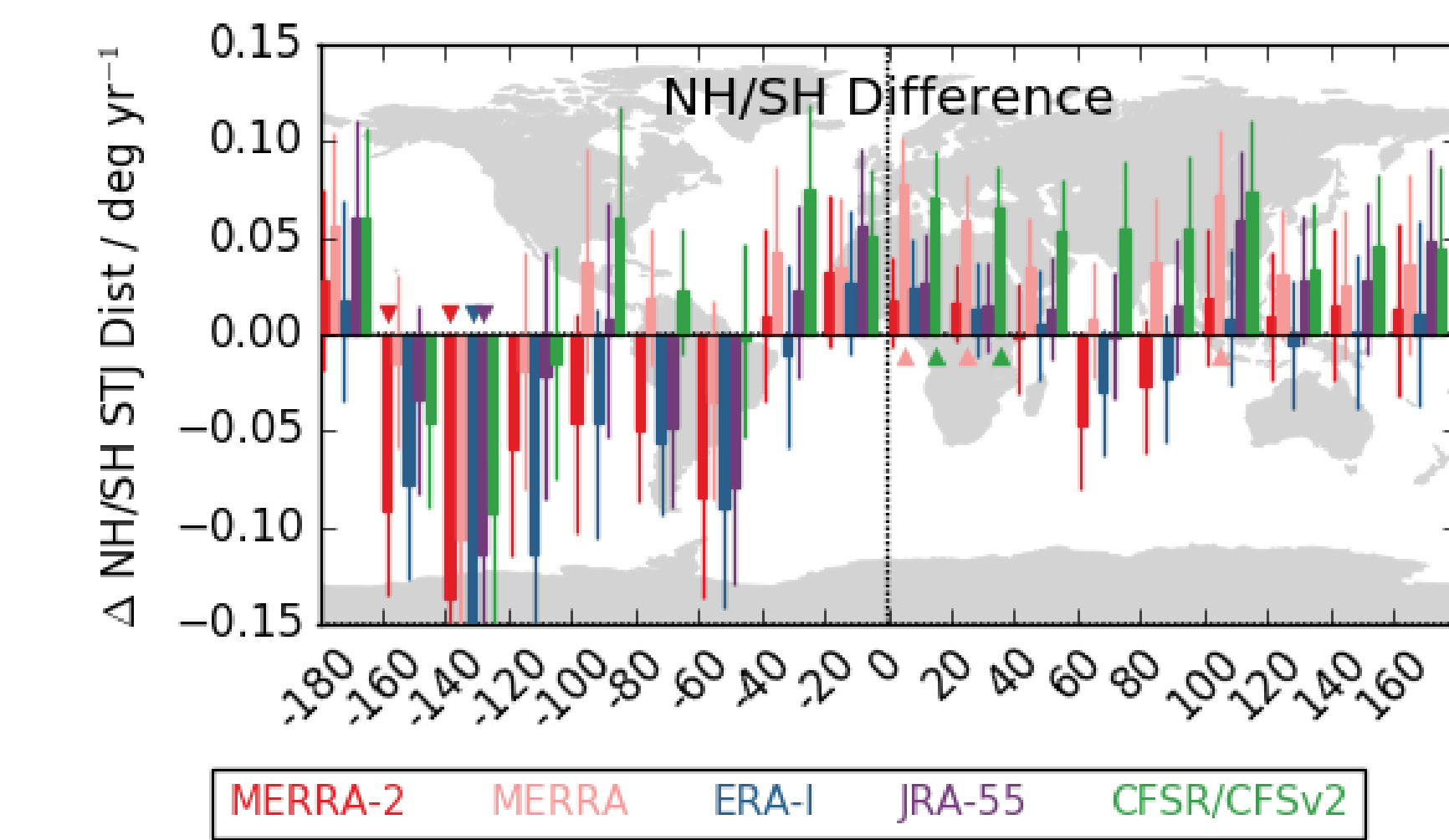


Figure 9: Changes in latitude difference between NH and SH STJ from 1979 through 2014, by longitude region for DJF (adapted from Manney and Hegglin, 2018).

Correlations of the STJ with ENSO (Figures 10 and 11) and QBO (as well as other natural modes of variability) may explain some of the jet changes.

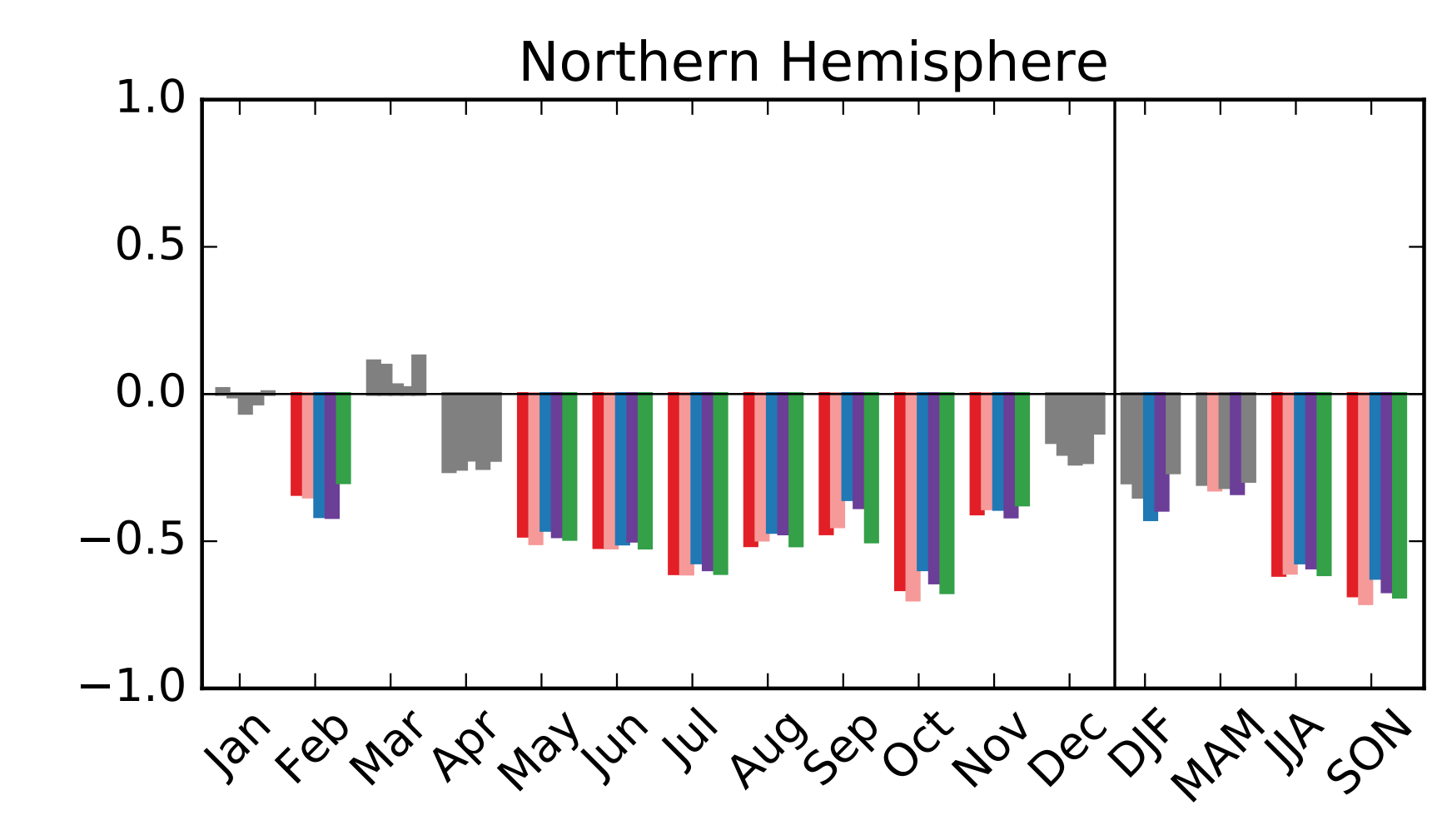


Figure 10: STJ Correlations with ENSO (MEI Index) by month and season for 1980 through 2015. Colored bars are significant at the 95% confidence level determined by a bootstrapping analysis. (Manney et al., 2019a, in preparation.)

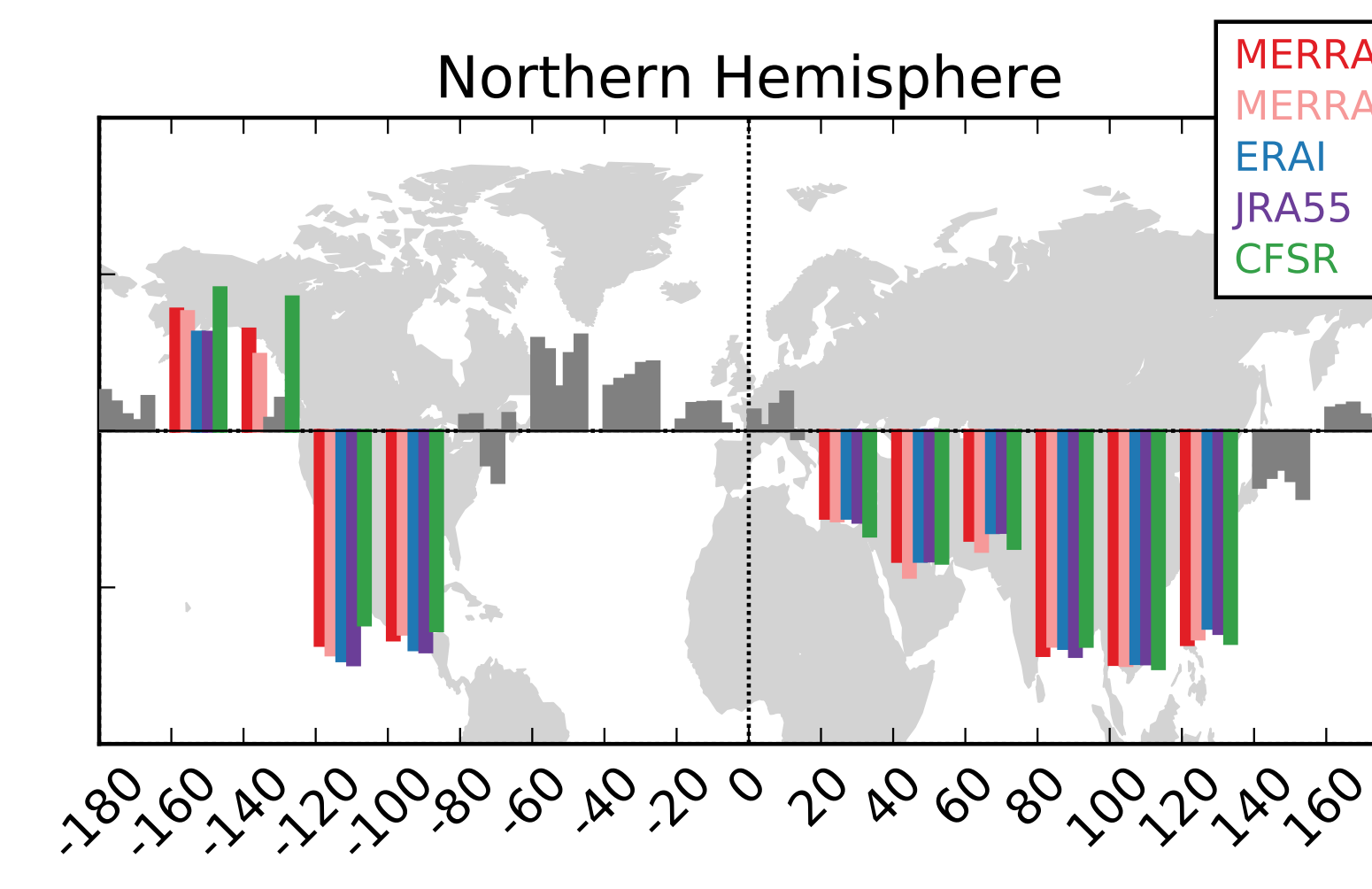


Figure 11: STJ Correlations with ENSO for DJF by longitude region. (Manney et al., 2019a, in preparation.)

Jet correlations with ENSO and QBO are in turn associated with ozone variability in relation to the STJ Olsen et al. (2019) showed ozone variability explained by ENSO and QBO in relation to the STJ (also see Olsen et al., poster #23 at this session, for further details):

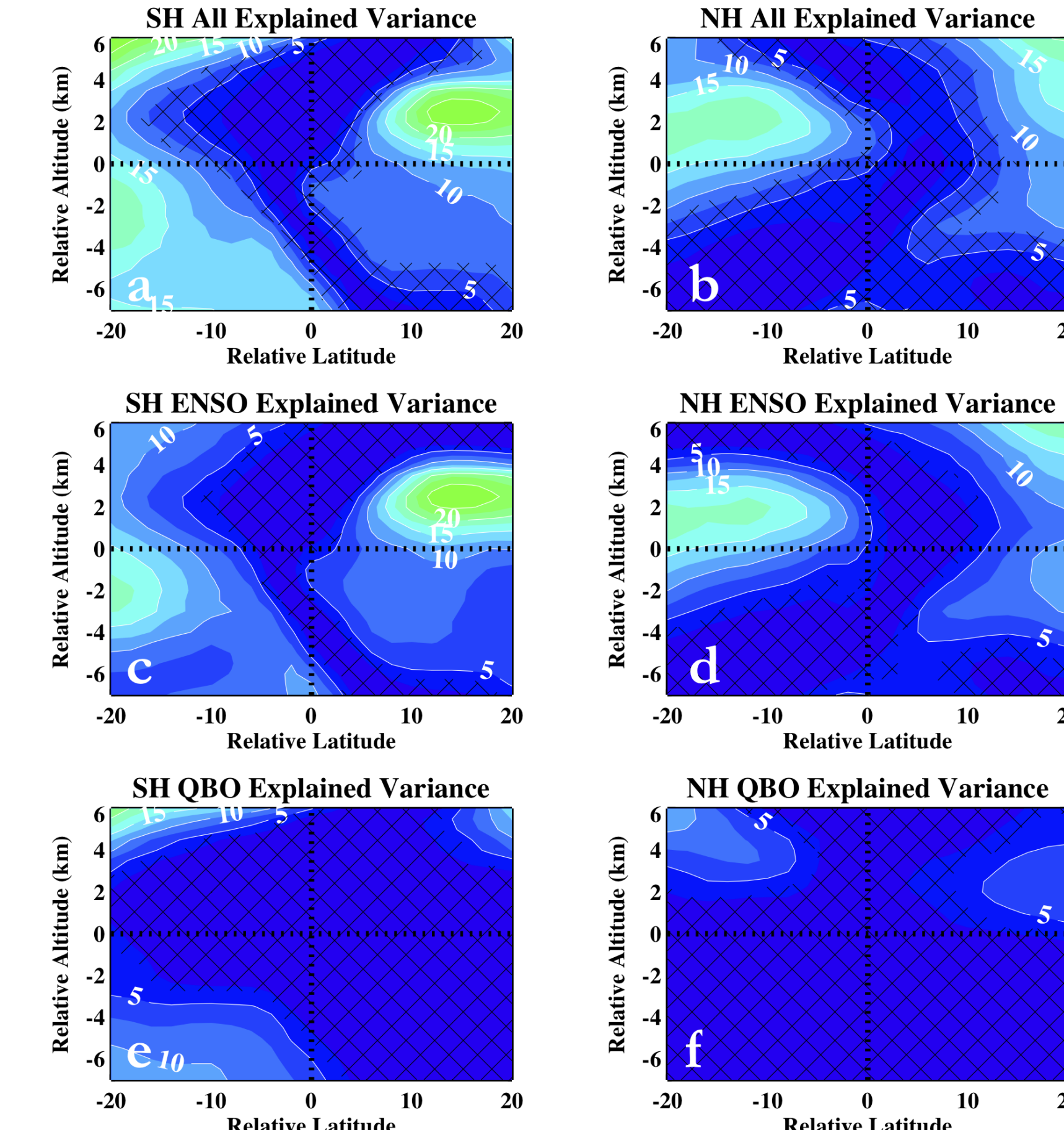


Figure 12: Ozone variance explained by ENSO and QBO (top panels) and ENSO (center) and QBO (bottom) individually (Olsen et al., 2019, Figure 4).

References

Davis, S. M., and Coauthors, 2017: Assessment of upper tropospheric and stratospheric water vapour and ozone in reanalyses. *Atmos. Chem. Phys. Disc.*, submitted.

Manney, G. L., and M. I. Hegglin, 2018: Seasonal and regional variations in long-term changes in upper tropospheric jets from reanalyses. *J. Clim.*, **31**, 423–448.

Manney, G. L., M. I. Hegglin, W. H. Daffer, M. J. Schwartz, M. L. Santee, and S. Pawson, 2014: Climatology of upper tropospheric/lower stratospheric (UTLS) jets and tropopauses in MERRA-2. *J. Clim.*, **27**, 3248–3271.

Manney, G. L., Z. D. Lawrence, and M. I. Hegglin, 2019a: Interannual variability in upper tropospheric jets in reanalyses: Relationships to ENSO, to be submitted to *J. Clim.*, 2019.

Manney, G. L., Z. D. Lawrence, M. L. Santee, M. J. Schwartz, and K. Wargan, 2019b: A moments view of climatology and variability of the Asian monsoon anticyclone, in preparation, to be submitted to *J. Clim.*, 2019.

Manney, G. L., and Coauthors, 2011: Jet characterization in the upper troposphere/lower stratosphere (UTLS): Applications to climatology and transport studies. *Atmos. Chem. Phys.*, **11**, 6115–6137.

Manney, G. L., and Coauthors, 2017: Reanalysis comparisons of upper tropospheric/lower stratospheric jets and multiple tropopauses. *Atmos. Chem. Phys.*, **17**, 5411–5426.

Olsen, M. A., G. L. Manney, and J. Liu, 2019: The ENSO and QBO impact on ozone variability and stratosphere-troposphere exchange relative to the subtropical jets. *J. Geophys. Res.*, **124** (13), 7379–7392, doi:10.1029/2019JD030435, URL <https://agupubs.onlinelibrary.wiley.com/doi/abs/10.1029/2019JD030435>.

Schwartz, M. J., G. L. Manney, M. I. Hegglin, N. J. Livesey, M. L. Santee, and W. H. Daffer, 2015: Climatology and variability of trace gases in extratropical multiple tropopause regions from MLS, HIRDLS and ACE-FTS measurements. *J. Geophys. Res.*, **120**, 843–867, doi:10.1002/2014JD021964.

Xian, T., and C. R. Homeyer, 2019: Global tropopause altitudes in radiosondes and reanalyses. *Atmos. Chem. Phys.*, **19**, 5661–5678.